

# MASS SPECTROMETRY AT 100 PARTS PER TRILLION

DAVID E. PRITCHARD AND JAMES K. THOMPSON

*Department of Physics and Research Laboratory of Electronics,  
Massachusetts Institute of Technology,  
Cambridge, Massachusetts, USA, 02139*

## 1. Abstract

Using a Penning trap single ion mass spectrometer, we have measured the atomic masses of 13 isotopes, many important for fundamental metrology and fundamental constants [9] [16] [3]. The fractional accuracy of the measurements,  $\approx 10^{-10}$ , is typically two orders of magnitude better than previously accepted values. This paper provides an overview of the MIT Penning trap measurements with special emphasis on the new techniques which we have developed for making measurements with accuracy  $10^{-10}$ . We go on to discuss some current work and proposals for improving the accuracy by another order of magnitude. We conclude with a discussion of the scientific payoff already realized, and the future scientific applications of precision mass spectrometry.

## 2. Introduction and Overview

Accuracy in mass spectrometry has been advanced over two orders of magnitude by the use of resonance techniques to compare the cyclotron frequencies of single trapped ions. This paper provides an overview of the MIT Penning trap measurements with special emphasis on the new techniques which we have developed for making measurements with accuracy  $10^{-10}$ . We go on to discuss some current work and proposals for improving the accuracy by another order of magnitude. We conclude by describing the scientific payoff already realized, as well as further scientific applications. It should be noted that in addition to our work at a part in  $10^{10}$  accuracy, R. Van Dyck's group at the University of Washington has performed measurements of 7 atomic species with accuracies of several parts in  $10^{10}$  [19] [18]. Their results for the same ions agree satisfactorily with our results.

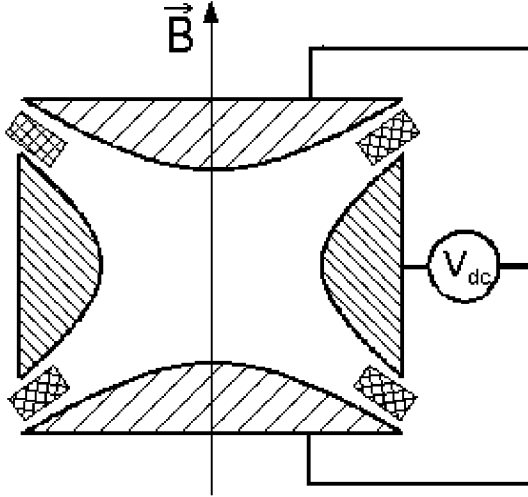


*Figure 1.* Hyperbolic Penning Trap cross section. A large magnetic field provides radial confinement. The electrodes are hyperbolae of rotation and form the equipotentials of a weak quadrupole electric field which provides a harmonic restoring force along the magnetic field lines. Guard ring electrodes located on the hyperbolic asymptotes are adjusted to approximately  $V_{dc}/2$  in order to minimize the lowest order non-quadrupole electric field component. At rf frequencies, the guard rings are split in order to provide dipole cyclotron drives and quadrupole mode couplings.

### 3. MIT Penning Trap

Experimentally, we compare the masses of two ions by alternately measuring their cyclotron frequencies (which are inversely proportional to the masses) in a large and highly-uniform magnetic field (8.5T) from a superconducting magnet. A single ion is held in a small region of space by the magnetic field, which provides radial confinement, and by an additional weak dc quadrupole electric field which provides axial confinement. This combination of confining fields is known as a Penning trap. Trapping the ion allows the long observation time necessary for high precision. Using a single ion is crucial for high accuracy since this avoids the frequency perturbations caused by the coulomb interaction between multiple ions.

The combination of magnetic and electric fields in our Penning trap results in three normal modes of motion: trap cyclotron, axial, and magnetron, with frequencies  $\omega'_c/2\pi \approx 5 \text{ MHz} \gg \omega_z/2\pi \approx 0.2 \text{ MHz} \gg \omega_m/2\pi \approx 0.002 \text{ MHz}$ , respectively. The free-space cyclotron frequency  $\omega_c$  is recovered from the quadrature sum of the three normal mode frequencies (invariant with respect to trap tilts and ellipticity[4]).

### 3.1. SQUID DETECTOR

We have developed ultrasensitive superconducting electronics to detect the miniscule currents ( $\leq 10^{-14}$  amperes) that a single ion's axial motion induces in the trap electrodes. The detector consists of a dc SQUID coupled to a hand wound niobium superconducting resonant transformer ( $Q \approx 4 \times 10^4$ ) connected across the endcaps of the Penning trap [21]. Our detection noise is currently dominated by the 4 K Johnson noise present in the resonant transformer- a fact we have exploited as discussed later. Energy loss in the resonant transformer damps the axial motion at a rate  $\gamma_z/2\pi \sim 1$  Hz quickly bringing the axial motion to thermodynamic equilibrium at 4 K.

### 3.2. MODE COUPLING AND $\pi$ -PULSES

The axial oscillation frequency of any ion can be tuned into resonance with the fixed detector frequency by changing the dc trapping voltage. The trap cyclotron and magnetron motions can then be detected by coupling them to the axial motion via a resonant quadrupole rf coupling[7]. This coupling causes the two modes to cyclically and phase coherently exchange their classical actions (amplitude squared times frequency). In analogy to the Rabi problem, a  $\pi$ -pulse can be created by applying the coupling just long enough to cause the coupled modes to exactly exchange their actions.

### 3.3. PULSE AND PHASE: COMPARING SIMILAR MASSES

We have developed the Pulse and Phase (abbreviated PNP) method to achieve cyclotron measurement precisions of  $10^{-10}$  in less than 1 minute [6]. A PNP measurement starts by cooling the trap cyclotron mode via coupling to the damped axial mode. The trap cyclotron motion is then driven or pulsed to a reproducible amplitude and phase at  $t = 0$  and then allowed to accumulate phase for some time T, after which a  $\pi$ -pulse is applied. The phase of the axial signal immediately after the  $\pi$ -pulse is then measured with rms uncertainty of order 10 degrees. Because of the phase coherent nature of the coupling, this determines the cyclotron phase with the same uncertainty. The trap cyclotron frequency is determined by measuring the accumulated phase versus evolution time T with the shorter times allowing the measured phase (which is modulo 360 degrees) to be properly unwrapped (see Fig.2). The PNP method is particularly suited to measure mass doublets- pairs of species such as  $\text{CD}_4^+$  and  $\text{Ne}^+$  that have the same total atomic number. Having the same mass to  $< 10^{-3}$  makes these comparisons insensitive to many systematic instrumental effects.

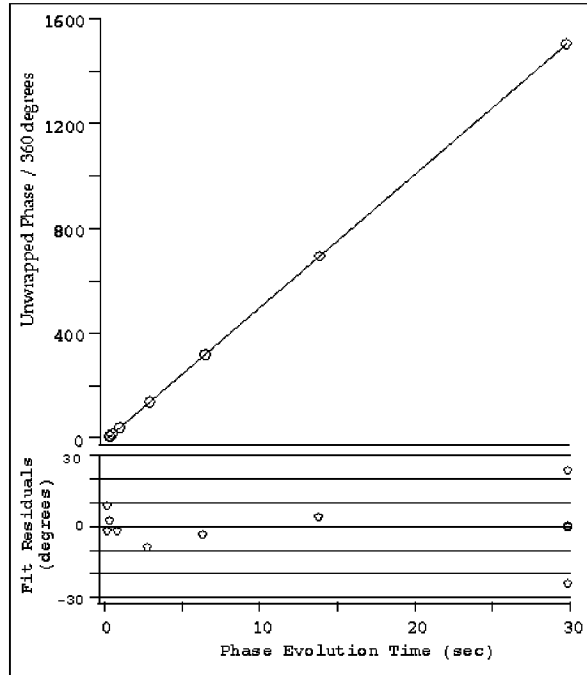


*Figure 2.* PNP Cyclotron Frequency Measurement: cyclotron phase measured versus phase evolution time and residuals from linear fit. The cyclotron phase accumulated by a single  $C_2^+$  is measured modulo 360 degrees and must then be unwrapped using shorter phase evolution times to extrapolate to longer times. The phase unwrapping is computationally simplified by frequency mixing the detected phase to approximately 50 Hz. The lower plot shows the residuals from the linear fit in degrees. The short time rms phase scatter is typically 10 degrees while the longer time points display frequency noise due to magnetic field fluctuations.

### 3.4. SOF: COMPARING DISSIMILAR MASSES

#### 3.4.1. Comparing non-doublets

To compare an ion to  $^{12}C$ , it is crucial to determine the masses of  $^1H$  and  $D$  ( $^2H$ ) so that they can be combined with  $^{12}C$  to form doublet comparison molecules (for instance  $O^+/CH_4^+$  and  $Ne^+/CD_4^+$ ) since comparing near equal masses reduces the size of many experimental systematic errors. Therefore, it is crucial to determine the masses of  $^1H$  and  $D$ . However, there are very few routes for doing this with doublet comparisons and even fewer direct routes involving a single mass doublet comparison.

To illustrate why it is difficult to find a series of doublet mass ratios which yield masses of  $^1H$  and  $D$ , consider the set of comparisons (i.e. mass ratios)

$$\frac{\text{N}^+}{\text{CH}_2^+} \quad , \quad \frac{\text{O}^+}{\text{CH}_4^+} \quad , \quad \frac{\text{CO}^+}{\text{N}_2^+}$$

which would seem to determine the three unknown atomic masses H, N and O (i.e. relative to C). A doublet mass ratio is so close to 1 that it should be thought of as determining a mass difference. For example, if  $R \equiv \text{N}^+/\text{CH}_2^+$  then

$$\text{N}^+ - \text{CH}_2^+ \approx (R - 1)(\text{CH}_2^+)' = \Delta M < 0.001 \times (\text{CH}_2^+)'$$

where the mass  $(\text{CH}_2^+)'$  is known from other experiments with several orders of magnitude less accuracy. From this perspective and after correcting for ionization and molecular binding energies, the above set of measured cyclotron frequency ratios determine the mass differences

$$\begin{aligned} \text{N} - \text{C} - 2\text{H} &= \Delta M_1 \\ \text{O} - \text{C} - 4\text{H} &= \Delta M_2 \\ \text{O} + \text{C} - 2\text{N} &= \Delta M_3. \end{aligned}$$

Unfortunately, it is clear that these relations yield only 2 linearly independent equations— combining the first two equations yields the third which therefore is a consistency check on the three measurements. Using non-doublet ratios such as  $\text{CD}_4^+/\text{C}^+$  and  $\text{CH}_4^+/\text{C}^+$  removes such singularities from the matrix relating neutral atomic masses to measured mass differences.

### 3.4.2. *Separated Oscillatory Fields*

In the case of a non-doublet comparison, the difference in the trapping voltages needed to detect each ion's axial motion is large enough to cause significant shifts in the ion's equilibrium position due to charge patches on the trap electrodes. The shift in equilibrium position causes a systematic error because of magnetic field inhomogeneities.

We have developed the SOF (separated oscillatory field) technique [16] to allow us to make cyclotron frequency comparisons using the same trapping voltage during the phase evolution time. An SOF sequence is identical to the PNP sequence but with a second drive pulse equal in strength to the first in place of the  $\pi$ -pulse. If the second drive pulse is in (out of) phase with the cyclotron motion, the two drive pulses add (subtract) resulting in a large (small) cyclotron amplitude. The result is that the cyclotron's phase information is encoded in the cyclotron amplitude. The trapping voltages can be adiabatically adjusted for axial detection and a  $\pi$ -pulse then

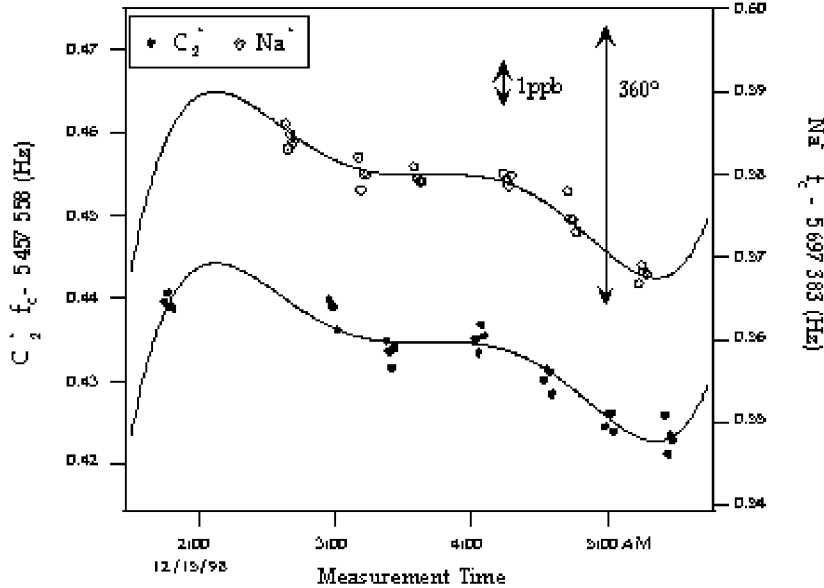


*Figure 3.*  $\text{Na}^+/\text{C}_2^+$  Cyclotron Frequency Ratio Measurement. We trapped each ion and measured the cyclotron frequency four times before expelling it and repeating the procedure for the other ion. In order to remove long term drift of the magnetic field and extract a frequency ratio, a fourth order polynomial and frequency difference were simultaneously fit to the combined set of cyclotron frequency measurements as shown by the solid line. For scale, the arrows indicate the frequency intervals corresponding to a 1 ppb frequency change and a 360 degree phase unwrap error.

applied. The detected axial amplitude versus phase evolution time  $T$  produces a classical Ramsey fringe which oscillates at the difference between the drive and trap cyclotron frequencies.

### 3.5. ANALYSIS: MAKING A MASS TABLE

A cyclotron frequency ratio of two different ions is determined by a run measuring a cluster of  $\omega_c$  values for an ion of type A, then for type B, etc. In a typical 4-hour run period (from 1:30-5:30 am when the nearby electrically-powered subway is not running), we can typically record between 5 and 10 alternations of ion type (see Fig. 3).

Since the measured free-space cyclotron frequencies exhibit a common slow drift, we fit a polynomial plus a frequency difference to the combined set of cyclotron frequency measurements for the night. The average polynomial fit order is typically between 3 and 5 and is chosen using the F-test

criterion [1] as a guide to avoid removing frequency changes which are not correlated between ion types. The distribution of residuals from the polynomial fits has a Gaussian center with a standard deviation  $\sigma_{resid} \approx 0.25$  ppb and a background ( $\approx 2\%$  of the points) of non-Gaussian outliers [9]. We handle these non-Gaussian outliers using a robust statistical method to first properly describe the observed statistical distribution of data points and then to smoothly deweight the nongaussian points[13], [9].

In all, we have measured a set of 28 cyclotron frequency ratios during 55 night runs. We correct these ratios for binding energies to arrive at a set of measured linear mass difference equations as described in section 3.4.1. The measured ratios were chosen so that at least two completely independent sets of mass ratios enter into the determination of each atomic mass. Performing a global least square fit to these linear equations yields the neutral masses in Table 1 with an overall  $\chi^2_\nu = .83$  indicating excellent internal consistency. Other experimental checks on errors include measuring calculable mass to charge ratios (i.e.  $\text{Ar}^{++}/\text{Ar}^+$ ) and measuring redundant mass ratios at different mass to charge ratios which would have very different systematic errors (i.e.  $\text{O}^+/\text{CH}_4^+$ ,  $\text{CO}^+/\text{C}_2\text{H}_4^+$ , and  $\text{CO}_2^+/\text{C}_3\text{H}_8^+$  all determine the same mass difference  $\text{C} + 4\text{H} - \text{O}$  at  $m/q = 16, 28,$  and  $44$ ).

## 4. Towards Higher Precision

### 4.1. SIMULTANEOUS CYCLOTRON MEASUREMENTS

Using either of the measurement techniques above, a typical phase accumulation time of 1 minute yields a precision of  $\approx 1 \times 10^{-10}$  and an irreproducibility of  $\sim 2.5 \times 10^{-10}$  due to short term fluctuations of the magnetic field. The typical precision with which we can compare the cyclotron frequencies of two ions ( $\approx 1 \times 10^{-10}$  after  $\sim 12$  alternations) is limited mainly by magnetic field drift while alternating ion types (typical time scales of 5 to 15 minutes). Making simultaneous cyclotron frequency measurements of the two ions would lead to much higher precision.

We have proposed a technique [5] in which we would trap the two ions of interest in the same trap at the same time so that we could perform simultaneous cyclotron frequency measurements. In theory, it should be possible to place the ions on a common magnetron motion so that they follow each other around the center of the trap and thus sample the same magnetic field. At a separation distance of  $\sim 1$  mm, the systematic shift of the cyclotron frequency ratio is predicted to be less than a part in  $10^{11}$ .

A second technique of interest is to have two axially adjacent traps with one ion in each trap. By swapping ions between traps we could cancel systematic the difference in the magnetic fields at the two trap centers. This technique also has predicted systematic errors below a part in  $10^{11}$  [5].

TABLE 1. Measured neutral masses[9], [3]. The error in the last digits is in parenthesis. The last two columns give the fractional accuracy of the measurements in ppb (parts in  $10^9$ ) and the improvement in accuracy over pre-Penning Trap mass values (from the 1983 atomic mass evaluation [20]). Note that the mass of the neutron is determined from the masses of  $^1\text{H}$  and  $^2\text{H}$  combined with measurements of the deuteron binding energy which has recently been improved [14].

Species	MIT Mass (u)	ppb	$\frac{\sigma_{MIT}}{\sigma_{83}}$
$^1\text{H}$	1.007 825 031 6 (5)	0.50	24
n	1.008 664 923 5 (23)	2.28	6
$^2\text{H}$	2.014 101 777 9 (5)	0.25	48
$^{13}\text{C}$	13.003 354 838 1 (10)	0.08	17
$^{14}\text{N}$	14.003 074 004 0 (12)	0.09	22
$^{15}\text{N}$	15.000 108 897 7 (11)	0.07	36
$^{16}\text{O}$	15.994 914 619 5 (21)	0.13	24
$^{20}\text{Ne}$	19.992 440 175 4 (23)	0.12	957
$^{23}\text{Na}$	22.989 769 280 7 (28)	0.12	93
$^{28}\text{Si}$	27.976 926 532 4 (20)	0.07	350
$^{40}\text{Ar}$	39.962 383 122 (33)	0.08	424
$^{85}\text{Rb}$	84.911 789 732 (14)	0.16	193
$^{87}\text{Rb}$	86.909 180 520 (15)	0.17	187
$^{133}\text{Cs}$	132.905 451 931 (27)	0.20	111

## 4.2. SQUEEZING

The finite temperature of the cyclotron mode causes variation of the amplitude from one PNP sequence to the next. This shot-to-shot amplitude noise results in a shot-to-shot variation of the cyclotron frequency reflecting the mass change expected from special relativity (magnetic field inhomogeneities also shift the cyclotron frequency). The cyclotron frequency variation due to special relativity is expected to be several parts in  $10^{11}$  for  $m/q \sim 20$  and close to a part in  $10^{10}$  for lighter species such as  $^3\text{He}$  and  $^3\text{H}$ .

In analogy to squeezed states of light, we have demonstrated a technique in which a parametric drive at  $2 \times \omega_z$  produces quadrature squeezing of the



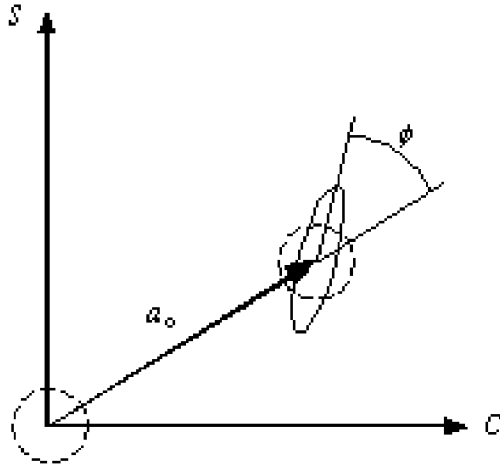


*Figure 4.* Squeezing of Thermal Distribution. The finite temperature of the ion's cyclotron mode results in shot-to-shot variation of the cyclotron amplitude and phase after the initial drive pulse (indicated by  $a_0$ ) of a PNP or SOF sequence. The isotropic thermal uncertainty (dashed circle) can be squeezed (ellipse) before the drive pulse to reduce either the amplitude ( $\phi = 90$ ) or the phase ( $\phi = 0$ ) uncertainty. Amplitude squeezing is more advantageous for mass measurements because amplitude fluctuations lead to shot-to-shot cyclotron frequency fluctuations due to special relativity and magnetic field inhomogeneities.

axial thermal uncertainty (Fig. 4) [17]. The squeezed thermal distribution can then be swapped into the cyclotron mode using a  $\pi$ -pulse. By properly adjusting the relative phase of the parametric drive and the cyclotron drive, we have demonstrated a factor of 2 reduction in the amplitude fluctuations[17]. We have also proposed two other techniques combining squeezing with selective anaharmonicities [8] that should achieve amplitude squeezing by at least a factor of 5.

#### 4.3. ELECTRONIC REFRIGERATION

We have been able to use feedback to reduce the effective temperature of the superconducting transformer used to detect the ion's axial motion below the ambient 4 K. This is possible because the quiet dc SQUID allows us to accurately measure the 4 K Johnson noise in the transformer and to add negative feedback to reduce the noise (Fig. 5) [11]. The negative feedback reduces the transformer voltage across the trap which is responsible for damping the ion's axial motion. The S/N is improved because the ion damps more slowly thus allowing a longer signal averaging time. Restating this, even though the ratio of instantaneous ion current to Johnson noise current remains unchanged by the feedback, the ion's signal is made more

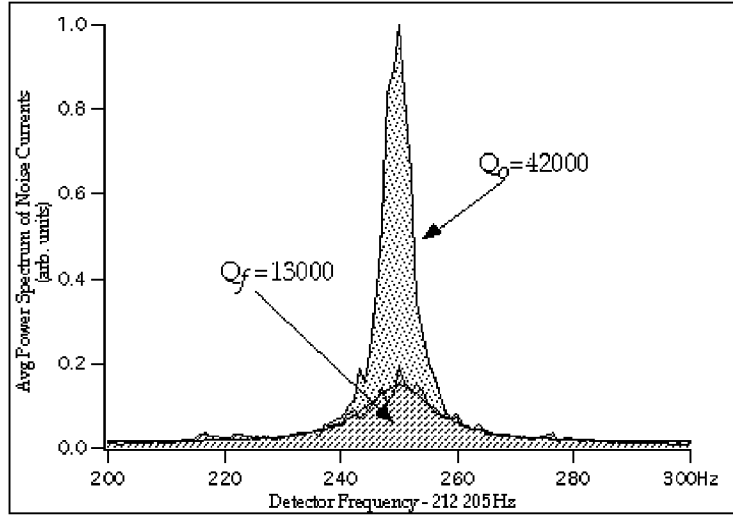


*Figure 5.* Electronic Refrigeration of Noise Currents. The average power spectrum of the detected Johnson noise current in the superconducting resonant transformer with and without negative feedback. In this example, both the  $Q$  and effective electronic temperature (which is just proportional to the area under the curves) are reduced by a factor of 3. In addition to improved signal to noise, this also results in a colder ion because the ion comes to thermodynamic equilibrium with the subthermal noise currents.

monochromatic and can be detected with higher S/N against the broadband Johnson noise background. The increased S/N has improved our ability to measure the ion's axial frequency, phase, and amplitude by factors of  $\sim 4$ , 2, and 2 respectively.

A further benefit of this electronic refrigeration is that the ion comes to thermodynamic equilibrium with the subthermal transformer resulting in a colder ion as well. This should reduce the shot-to-shot cyclotron frequency fluctuations described in section 4.2. The present ratio of dc SQUID noise to the transformer's Johnson noise currently sets a rough upper limit of reducing the transformer's effective temperature by a factor of  $\sim 9$  and thus the shot-to-shot relativistic cyclotron frequency noise by  $\sim 3$ .

## 5. Scientific Applications

To date we have measured a total of 13 neutral masses, ranging from the mass of the proton to the mass of  $^{133}\text{Cs}$  all with accuracies one to three orders of magnitude higher than the previously accepted values. This advance in accuracy has and will allow important contributions in both fundamental physics and metrology, including:

- an 80-fold improvement of the current  $\gamma$ -ray wavelength standard by using  $E = \Delta mc^2$  to determine the energies of  $^{14}\text{N}$  neutron capture  $\gamma$ -rays (widely used as  $\gamma$ -ray calibration lines)[9],
- opening the way for an atomic standard of mass by replacing the artifact kilogram mass standard with a crystal of pure silicon and our accurate determination of the atomic mass of  $^{28}\text{Si}$  [9],
- new determinations of the molar Planck constant,  $N_A h$ , with precision  $\sim 10$  ppb [3],
- new determinations of the fine structure constant,  $\alpha$ , with precision  $\sim 5$  ppb [3],
- providing reference masses for mass measurements of radioactive nuclei which are important for testing models of astrophysical heavy element formation [10].

Improvements in accuracy will allow further contributions to fundamental physics including:

- measurement of the  $^3\text{H} - ^3\text{He}$  mass difference, which is important in ongoing experiments to determine the electron neutrino rest mass [2] [15],
- checking the relationship  $E = mc^2$  to a few parts in  $10^7$  by weighing  $\gamma$ -rays from neutron capture by  $^{32}\text{S}$  [12]; this will also provide an independent determination of  $N_A h$  and the fine structure constant  $\alpha$ ,
- determination of excitation and binding energies of atomic and molecular ions by weighing the associated small decrease in mass,  $\Delta m = E_{\text{binding}}/c^2$  (we must reach our ultimate goal of a few parts  $10^{12}$  to make this a generally useful technique),
- improvement of traditional applications of mass spectrometry resulting from our orders of magnitude improvement in both accuracy and sensitivity.

This work is supported by the National Science Foundation, a NIST Precision Measurements Grant, and was formerly supported by the Joint Services Electronics Program.

## References

1. Bevington, P. and D. Robinson: 1992, *Data Reduction and Error Analysis for the Physical Sciences*. Boston: McGraw-Hill, 2nd edition.
2. Bonn, J., B. Bornschein, L. Bornschein, L. Fickinger, O. Kazachenko, A. Kovalik, C. Kraus, E. W. Otten, H. Ulrich, and C. Weinheimer: 2000, 'Newest results from the Mainz neutrino-mass experiment'. *Phys. Atom. Nuclei* **63**(6), 969–974.
3. Bradley, M. P., J. V. Porto, S. Rainville, J. K. Thompson, and D. E. Pritchard: 1999, 'Penning trap measurements of the masses of Cs-133, Rb-87, Rb- 85, and Na-23 with uncertainties  $\leq 0.2$  ppb'. *Phys. Rev. Lett.* **83**(22), 4510–4513.
4. Brown, L. S. and G. Gabrielse: 1986, 'Geonium Theory - Physics of a Single Electron or Ion in a Penning Trap'. *Rev. Mod. Phys.* **58**(1), 233–311.

5. Cornell, E. A., K. R. Boyce, D. L. K. Fyngenson, and D. E. Pritchard: 1992, '2 Ions in a Penning Trap - Implications for Precision Mass- Spectroscopy'. *Phys. Rev. A* **45**(5), 3049–3059.
6. Cornell, E. A., R. M. Weisskoff, K. R. Boyce, R. W. Flanagan, G. P. Lafyatis, and D. E. Pritchard: 1989, 'Single-Ion Cyclotron-Resonance Measurement of  $M(\text{Co}^+)M(\text{N}2^+)$ '. *Phys. Rev. Lett.* **63**(16), 1674–1677.
7. Cornell, E. A., R. M. Weisskoff, K. R. Boyce, and D. E. Pritchard: 1990, 'Mode-Coupling in a Penning Trap - Pi-Pulses and a Classical Avoided Crossing'. *Phys. Rev. A* **41**(1), 312–315.
8. Difilippo, F., V. Natarajan, K. R. Boyce, and D. E. Pritchard: 1992, 'Classical Amplitude Squeezing for Precision-Measurements'. *Phys. Rev. Lett.* **68**(19), 2859–2862.
9. Difilippo, F., V. Natarajan, K. R. Boyce, and D. E. Pritchard: 1994, 'Accurate Atomic Masses for Fundamental Metrology'. *Phys. Rev. Lett.* **73**(11), 1481–1484.
10. Fogelberg, B., K. A. Mezilev, H. Mach, V. I. Isakov, and J. Slivova: 1999, 'Precise atomic mass values near Sn-132: The resolution of a puzzle'. *Phys. Rev. Lett.* **82**(9), 1823–1826.
11. Forward, R.: 1979, 'Electronic cooling of resonant gravity gradiometers'. *J. Appl. Phys.* **50**(1), 1.
12. Greene, G. L., M. S. Dewey, E. G. Kessler, and E. Fischbach: 1991, 'Test of Special Relativity by a Determination of the Lorentz Limiting Velocity - Does  $E = Mc^2$ '. *Phys. Rev. D* **44**(8), R2216 – R2219.
13. Huber, P.: 1981, *Robust Statistics*. New York: Wiley.
14. Kessler, E. G., M. S. Dewey, R. D. Deslattes, A. Henins, H. G. Borner, M. Jentschel, C. Doll, and H. Lehmann: 1999, 'The deuteron binding energy and the neutron mass'. *Phys. Lett. A* **255**(4-6), 221–229.
15. Lobashev, V. M.: 2000, 'Direct search for the neutrino mass in the beta decay of tritium: Status of the "Troitsk neutrino-mass" experiment'. *Phys. Atom. Nuclei* **63**(6), 962–968.
16. Natarajan, V., K. R. Boyce, F. Difilippo, and D. E. Pritchard: 1993, 'Precision Penning Trap Comparison of Nondoublets - Atomic Masses of H, D, and the Neutron'. *Phys. Rev. Lett.* **71**(13), 1998–2001.
17. Natarajan, V., F. Difilippo, and D. E. Pritchard: 1995, 'Classical Squeezing of an Oscillator for Subthermal Noise Operation'. *Phys. Rev. Lett.* **74**(15), 2855–2858.
18. Van Dyck RS, J., F. DL, Z. SL, and S. PB: 1998, 'High precision Penning trap mass spectroscopy and a new measurement of the proton's atomic mass'. In: *Trapped Charged Particles and Fundamental Physics.*, Vol. 457. Asilomar, CA, pp. 101–110, AIP.
19. Vandyck, R. S., D. L. Farnham, and P. B. Schwinberg: 1993, 'Tritium He-3 Mass Difference Using the Penning Trap Mass- Spectroscopy'. *Phys. Rev. Lett.* **70**(19), 2888–2891.
20. Wapstra, A. and G. Audi: 1985, 'The 1983 atomic mass evaluation. I. Atomic mass table.'. *Nuc Phys A* **A432**(1), 1–54.
21. Weisskoff, R. M., G. P. Lafyatis, K. R. Boyce, E. A. Cornell, R. W. Flanagan, and D. E. Pritchard: 1988, 'Rf Squid Detector for Single-Ion Trapping Experiments'. *J. Appl. Phys.* **63**(9), 4599–4604.